Environmental Science & Technology

pubs.acs.org/est Article

Isotopic Insights into Organic Composition Differences between Supermicron and Submicron Sea Spray Aerosol

Daniel R. Crocker,* Chathuri P. Kaluarachchi, Ruochen Cao, Julie Dinasquet, Emily B. Franklin, Clare K. Morris, Sarah Amiri, Daniel Petras, Tran Nguyen, Ralph R. Torres, Todd R. Martz, Francesca Malfatti, Allen H. Goldstein, Alexei V. Tivanski, Kimberly A. Prather, and Mark H. Thiemens

Cite This: *Environ. Sci. Technol.* 2022, 56, 9947−9958 Read Online

ABSTRACT: To elucidate the seawater biological and physicochemical factors driving differences in organic composition between supermicron and submicron sea spray aerosol (SSA_{super} and SSA_{sub}), carbon isotopic composition ($\delta^{13}C$) measurements were performed on size-segregated, nascent SSA collected during a phytoplankton bloom mesocosm experiment. The $\delta^{13}C$ measurements indicate that SSA_{super} contains a mixture of particulate and dissolved organic material in the bulk seawater. After phytoplankton growth, a greater amount of freshly produced carbon was observed in SSA_{super} with the proportional contribution being modulated by bacterial activity, emphasizing the importance of the microbial loop in controlling the organic composition of SSA_{super}. Conversely, SSA_{sub} exhibited no apparent relationship with biological activity but tracked closely with surface tension measurements probing the topmost ~0.2−1.5 μm of the sea surface microlayer. This probing depth is similar to a bubble's film thickness at the ocean surface, suggesting that SSA_{sub} organic composition may be influenced by the presence of surfactants at the air−sea interface that are transferred into SSA_{sub} by bubble bursting. Our findings illustrate the substantial impact of seawater dynamics on the pronounced organic compositional differences between SSA_{super} and SSA_{sub} and demonstrate that these two SSA populations should be considered separately when assessing their contribution to marine aerosols and climate.

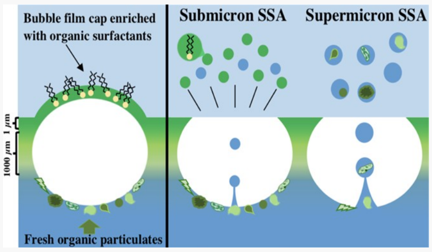

KEYWORDS: *sea spray aerosol, carbon isotopes, phytoplankton bloom, marine biogeochemistry, sea surface microlayer, marine aerosol source apportionment, ocean-aerosol organic transfer, surface tension*

1. INTRODUCTION

Atmospheric aerosols affect Earth's radiative budget directly by reflecting and absorbing incoming solar radiation and indirectly by serving as nuclei for water and ice cloud formation.[1] There is currently a large amount of uncertainty in aerosol radiative forcing estimates for the marine environment arising from the contribution of both natural and anthropogenic aerosols to the direct and indirect aerosol effects.[2,3] Sea spray aerosol (SSA), formed by bubbles bursting at the ocean surface, is often the most abundant primary aerosol type in the marine atmosphere.[4−6] However, as anthropogenic aerosol emissions have continued to increase above preindustrial levels, so has their contribution to marine aerosols.[7,8] The important role that SSA and anthropogenic aerosol play in marine cloud formation and climate necessitates methods that effectively characterize aerosol sources in the marine environment.[9,10]

Carbon isotope analysis ($\delta^{13}C$) is an excellent technique to distinguish between the fractional mass contribution of two carbon sources (e.g., marine-derived and continentally derived carbon). Many marine source apportionment studies assume that most of the aerosol carbon is contributed by primary emissions: SSA for marine-derived (f_{SSA}) and anthropogenic for continentally derived (f_{anth}).[11−16] This generalization does not account for secondary marine and terrestrial aerosols, but their carbon contributions are often lower than primary aerosols,[15] and this simplification is necessary to enable estimates of f_{anth} via a two-member isotopic mixing model (eq 1).

$$\delta^{13}C_{marine} = (f_{SSA})(\delta^{13}C_{SSA}) + (f_{anth})(\delta^{13}C_{anth}) \quad (1)$$

Equation 1 can differentiate between two carbon sources with distinct isotopic values but requires accurate knowledge of the $\delta^{13}C$ endmember values for both SSA ($\delta^{13}C_{SSA}$) and anthropogenic aerosol ($\delta^{13}C_{anth}$). Unfortunately, the $\delta^{13}C$ value for nascent SSA has been difficult to establish in the ambient environment due to background contributions from anthropogenic and terrestrial aerosols as well as the photo-

Received: March 28, 2022
Revised: June 14, 2022
Accepted: June 15, 2022
Published: June 28, 2022

chemical processing of primary SSA organic carbon (OC) during atmospheric transport.[17,18] Lacking a better option, initial source apportionment studies assumed that $\delta^{13}C_{SSA}$ had a uniform value equivalent to the global average $\delta^{13}C$ for surface ocean carbon, around −21‰.[11−13] More recent research contradicts this assumption, showing that marine aerosols have $\delta^{13}C$ values as high as −18 to −19‰ in oceanic regimes with elevated seawater biological activity.[15,19] These findings motivate further research aimed at understanding the biological and chemical factors influencing variability in nascent $\delta^{13}C_{SSA}$.

The organic material in SSA is derived from the two seawater carbon pools, dissolved and particulate organic carbon (DOC and POC), that are often operationally distinguished as material filterable/retained by a 0.7 μm GF/F filter. Thus, DOC consists primarily of single molecules, macromolecular structures, and small colloids, whereas POC is composed of phytoplankton and their detritus, large bacteria, and particulate aggregates.[20] The primary input of new organic material into the surface ocean occurs by phytoplankton carbon fixation, and most of this freshly produced OC is initially incorporated into the phytoplankton biomass.[21] This implies that freshly produced OC is initially present in the POC pool, which is further evidenced by ^{14}C measurements that show that surface ocean POC has a modern, "fresh" radiocarbon signature of around +100‰, whereas DOC is −200 to −400‰, indicating an older, more "aged" organic material.[22,23]

Harkening back to $\delta^{13}C_{SSA}$, the higher values observed under conditions of elevated biological activity can be attributed to biologically induced isotopic differences between freshly produced and aged OC. Oftentimes during large phytoplankton blooms, freshly produced OC is isotopically heavy (less negative $\delta^{13}C$) because the lack of CO_2 availability leads to less ^{12}C discrimination during CO_2 fixation.[24,25] Based upon this, researchers inferred that $\delta^{13}C_{SSA}$ values may reflect the proportional contribution to SSA from older, aged seawater carbon, consisting primarily of DOC, and newer, freshly produced seawater carbon that is mostly POC.[26] Their conclusion is supported by laboratory experiments on nascent SSA that combined $\delta^{13}C_{SSA}$ measurements with seawater $\delta^{13}C_{POC}$ and $\delta^{13}C_{DOC}$ measurements to reveal that increased biological activity leads to a greater incorporation of freshly produced OC in SSA, resulting in less negative $\delta^{13}C_{SSA}$ values.[27] The same study further illustrated the importance of accounting for variability in $\delta^{13}C_{SSA}$ values by demonstrating that assuming a constant $\delta^{13}C_{SSA}$ value of −21‰ can result in up to a 33% underestimation in the contribution of anthropogenic aerosol carbon to the marine environment.[27]

One remaining issue to address when comparing marine aerosol source apportionment studies is that some studies have measured total suspended particles (TSPs),[14,28] a combination of supermicron and submicron particles, while others have focused only on submicron particles.[15] This distinction is important because supermicron SSA (SSA_{super}) and submicron SSA (SSA_{sub}) often have dissimilar organic compositions due to their different formation mechanisms at the ocean surface.[29,30] The majority of SSA_{sub} are film drops produced when the bubble film cap bursts at the air−sea interface, whereas SSA_{super} is produced from an unstable jet formed at the bubble's base when the bubble cavity collapses.[6] Generally, SSA_{sub} contains aliphatic, surface-active dissolved organic material,[31,32] in accordance with its organic composition being heavily influenced by the sea surface microlayer (SSML), the top 1−1000 μm of the ocean surface containing elevated organic surfactant concentrations.[33,34] The organic composition of SSA_{super} is usually comparable to the underlying bulk seawater and often includes a large proportion of biological particulate material.[27,29,35] Logically, these organic composition differences may result in disparate $\delta^{13}C$ values for SSA_{super} and SSA_{sub} ($\delta^{13}C_{super}$ and $\delta^{13}C_{sub}$), but this possibility has yet to be explored.

Herein, we report values of $\delta^{13}C_{super}$ and $\delta^{13}C_{sub}$ for nascent SSA measured over the course of a phytoplankton bloom mesocosm experiment. The mesocosm experiment was conducted during the 2019 Sea Spray Chemistry And Particle Evolution (SeaSCAPE) study conducted in a unique ocean-atmosphere facility at the Scripps Institution of Oceanography (SIO).[36] The aim of this work is to identify key biological and physicochemical factors controlling the differences in organic composition and $\delta^{13}C$ values between SSA_{super} and SSA_{sub}.

2. MATERIALS AND METHODS

2.1. The Wave Channel Mesocosm Experiment. This work reports on a mesocosm phytoplankton bloom experiment conducted in a 33 m long ocean-atmosphere wave channel at the SIO Hydraulics Laboratory. A detailed diagram and comprehensive experimental description of this specific wave channel experiment can be found in Sauer et al.,[36] so here we have included a simplified depiction (Figure S1) and an overview of the experimental conditions and perturbations pertinent to the interpretation of our reported data. Similar to previous SSA experiments in the SIO wave channel, waves were generated using a hydraulic paddle, and a submerged fiberglass "beach" ramp was placed about midway down the channel to initiate wave breaking and SSA production.[32,35] To adapt the wave channel for atmospheric study, the top was covered from the paddle to 21 m downstream with acrylic panels backed by plywood and sealed with foam stripping. This isolated the wave breaking region as well as the aerosol sampling port from the ambient atmosphere (Figure S1). Particle-free air scrubbed of gaseous pollutants was also blown through the channel to carry nascent SSA to the sampling ports and reduce room air backflow. Background particle concentrations in the region preceding wave breaking were continuously monitored throughout the experiment by a condensation particle counter and were generally <5 cm^{-3}.[36] To enable phytoplankton growth, the transparent, glass side panels of the wave channel were lined with solar simulator lamps that provided photosynthetically active radiation (PAR) on a 14 hour/10 hour day/night diel cycle.

On July 23, 11,800 L of coastal Pacific Ocean seawater was collected from Scripps Pier, filtered with 50 μm Nitex mesh, and added to the wave channel. Overnight from July 25 to 26, a diluted (f/20) algae nutrient mixture with sodium metasilicate[37] was added dropwise to the wave channel to initiate phytoplankton growth. After nutrient addition, minimal phytoplankton growth was observed from July 26 to August 1, as indicated by chlorophyll-a (chl-a) measurements (see Section 2.2). Based on prior experience, it was known that initiating indoor phytoplankton blooms of this magnitude can be difficult, especially because the PAR flux from the solar simulator lamps (∼80 $\mu E\ m^{-2}$) is much lower than the typical solar PAR flux (>1000 $\mu E\ m^{-2}$).[38] In light of this, it was decided that inoculation with an already prosperous phytoplankton bloom may be necessary to stimulate

https://doi.org/10.1021/acs.est.2c02154
Environ. Sci. Technol. 2022, 56, 9947−9958

phytoplankton growth in the wave channel. Therefore, on July 28, a separate 1135 L carboy was filled with natural seawater collected and filtered in the same manner as the wave channel seawater above. A more concentrated f/2 algae nutrient mixture with sodium metasilicate was added to this seawater, and it was left outdoors to receive a higher PAR flux. When the carboy bloom reached exponential growth phase on August 1, as indicated by chl-a (Aquafluor, Turner Designs), and wave channel phytoplankton growth was still minimal, the decision was made to inoculate the wave channel with the carboy bloom. First, 1135 L of the wave channel seawater was removed, and then the carboy was added as a 10% inoculation along with more algae nutrients to bring the total wave channel nutrient concentration to f/2. The overall goal of this inoculation was to facilitate the growth of a robust phytoplankton bloom that would enable the investigation of biologically induced changes to the chemical composition of SSA.

2.2. *In Situ* Measurement of Chl-a and Dissolved CO_2 Concentrations. Phytoplankton bloom progression throughout the experiment was monitored by measuring chl-a. Chl-a is a widely applied proxy for phytoplankton biomass by both marine field studies[39,40] and mesocosm experiments[41−43] and was reported by all published work from the SeaSCAPE study to facilitate an easier comparison between data sets.[44−46] A flow-through sensor/analyzer suite was used for *in situ* measurements of bulk seawater properties including seawater temperature, dissolved oxygen, salinity, and chl-a (SeaBird Scientific SBE16 and SBE63 with Eco-Triplet BBFL2). The *in situ* chl-a data were calibrated using measurements of chl-a extracted from GF/F filtered bulk seawater and quantified by fluorometric analysis according to CalCOFI methods.[47]

A separate continuous flow system was used for the determination of the dissolved CO_2 concentration. This system measured pH (Honeywell Durafet) and dissolved oxygen (Aanderaa Data Instruments 3835 Optode) as well as pCO_2 and total dissolved inorganic carbon using a ″Burke-o-lator″ custom IR analyzer.[48,49] The seawater carbonate speciation and dissolved CO_2 concentration were calculated from these measurements with corrections made for seawater temperature and salinity.

2.3. Collection of Communal Bulk Seawater and SSML Samples. Each morning between 9 and 11 a.m., the bulk seawater and SSML were collected from the back of the wave channel in a designated seawater sampling section (Figure S1). Bulk seawater was siphoned into two 8 L Nalgene carboys using a 2 m Teflon tube placed about 20 cm below the seawater surface. All materials were successively rinsed three times with methanol, 70% ethanol, 10% HCl, and ultrapure water each day before collection. In the laboratory, all bulk seawater analyses used aliquots from the carboys to ensure that all measurements were made on comparable seawater samples.

The SSML was collected from the same seawater sampling section of the wave channel by employing the glass plate method.[50] The glass plate was carefully lowered into the water at a rate of 5−6 cm/s and withdrawn at the same rate, which corresponds to a sampled SSML thickness of around 50 μm.[50,51] After withdrawal from the seawater, the glass plate was suspended for 20 s to allow any bulk seawater to drain back into the wave channel. The remaining mixture of seawater and organics on the plate was considered the SSML and scraped into a combusted glass bottle using a Teflon scraper. This process was repeated, with ∼2 min between successive dips to allow for the reestablishment of the SSML,[52] until a 200 mL SSML volume had been collected.

2.4. SSML Surface Tension Measurements. Because of its strong attractive intermolecular forces, pure water has a high surface tension of about 72−73 mN m^{-1} at 25 °C, and pure seawater is even higher at 73−74 mN m^{-1}.[53] However, the strong attractive forces of water molecules can be disrupted by the presence of surfactants at the liquid surface, leading to a depression in surface tension. Therefore, surface tension measurements in seawater are often used to indicate the presence of surfactants.[54,55] In this study, two techniques were employed to measure the surface tension of SSML samples: a tensiometer and atomic force microscopy (AFM). The tensiometer measurements were made in triplicate with a Kibron AquaPi force tensiometer (Kibron, Finland) using the standard Du Noüy−Padday method.[56,57] Tensiometer measurements probe to a depth greater than 1000 μm into the solution and thus probe essentially the entirety of the SSML solution. Conversely, the AFM surface tension measurements are a newly developed technique capable of probing depths on the order of hundreds of nanometers.[58] Therefore, this measurement is representative of the topmost SSML layers that may contain more surface-active species. In this experiment, AFM force plot measurements were performed via the Molecular Force Probe 3D AFM (Asylum Research, Santa Barbara, CA) with high aspect ratio, constant diameter Ag_2Ga nanoneedles (NN-HAR-FM60, Nauga Needles). An SSML droplet was placed on a silicon wafer substrate, and force measurements were collected over the approximate center of the SSML droplet with a 1 Hz scan rate. The nanoneedle indented to a slightly variable probing depth in the SSML droplet, between 0.2 and 1.5 μm for our reported measurements; paused within the droplet for 2 s of dwell time; and then retracted away from the droplet with a constant pulling rate of 2 μm s^{-1}.[58] At least five consecutive force plots were collected for each sample, and the maximum retention force was used to quantify the droplet surface tension. Both the tensiometer and AFM nanoneedles were calibrated before and after each surface tension measurement by performing measurements on a reference ultrapure water droplet with known surface tension (72.8 mN m^{-1} at 25 °C). All surface tension data are reported as the mean with one standard deviation.

2.5. Seawater Analyses of Bacterial Concentration and Productivity. For the quantification of bacteria cells, bulk seawater samples were prepared according to standard protocols.[59,60] Samples were preserved with 5% glutaraldehyde, flash frozen with liquid nitrogen, and stored at −80 °C.[61] Bacteria samples were then diluted 10-fold in 1× TE buffer at pH 8 and stained for 10 min with SYBR Green I in the dark at room temperature.[59] Finally, bacteria cell enumeration was carried out using a BD FACSCanto II flow cytometer.

Bacterial production was measured daily in bulk seawater samples by [^{3}H]-leucine incorporation[62] modified for microcentrifugation.[63] Triplicate 1.7 mL aliquots were incubated with [^{3}H]-leucine (20 nM final concentration) for 1 h. Samples with 100% trichloroacetic acid added prior to [^{3}H]-leucine addition served as blanks. Leucine incorporation was converted to carbon production assuming 3.1 kg C (mol leucine)$^{-1}$.[64]

Bacterial carbon demand (BCD) is the sum of carbon incorporated into bacterial biomass (bacterial production) and carbon respired by bacteria back into CO_2 (bacterial respiration). An equation to estimate bacterial respiration

https://doi.org/10.1021/acs.est.2c02154
Environ. Sci. Technol. 2022, 56, 9947−9958

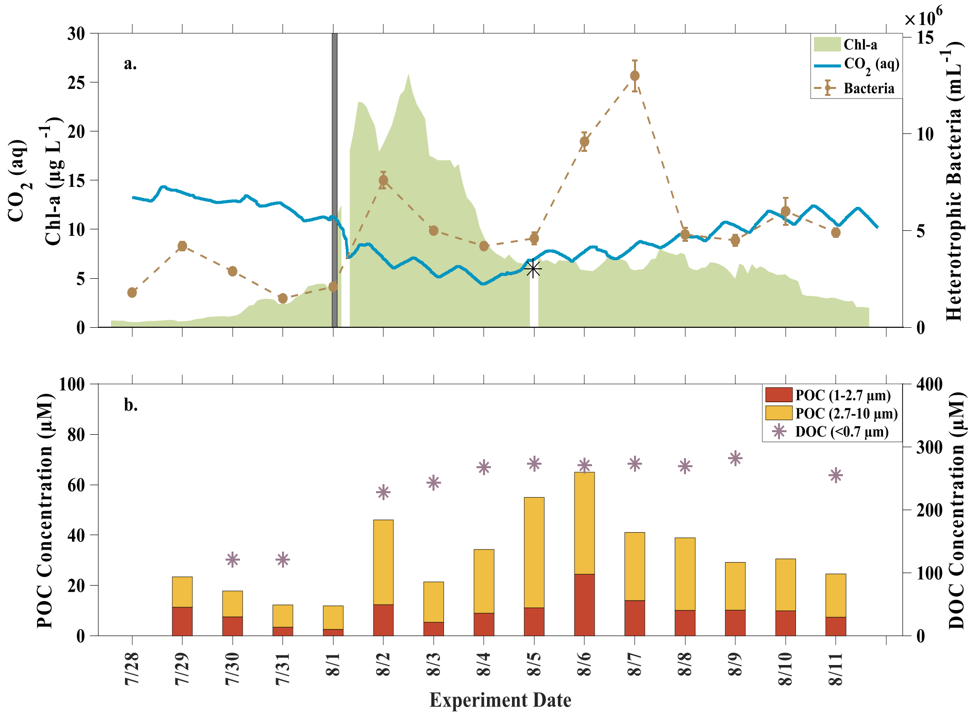

Figure 1. (a) Chl-a, dissolved CO_2, and bacteria concentrations throughout the mesocosm experiment. Dashed lines indicate individual measurements, while solid lines signify continuous sampling. The 10% inoculation on August 1 is indicated by the vertical gray line, and the asterisk denotes when the wave channel walls were scraped on August 5. (b) The DOC and POC_{1-10} concentrations during the experiment with the POC_{1-10} concentration (full bar height) separated into 1−2.7 μm (red) and 2.7−10 μm (yellow) size fractions. The POC_{1-10} measurement on August 1 represents the concentration before the 10% inoculation, while no analogous measurement was available for DOC.

from measured bacterial production was developed by del Giorgio and Cole (eq 2).[65]

$$\text{Bacterial respiration} = 3.70 \times (\text{bacterial production})^{0.41} \tag{2}$$

We used eq 2 to estimate bacterial respiration from daily bacterial production measurements and added these two values together to obtain the reported BCD values.

2.6. Collection and Filtration of POC and DOC Samples. One liter of bulk seawater from the carboys was used to collect POC samples segregated into two size classes, 1.0−2.7 and 2.7−10 μm, by three successive filtrations. First, the seawater was filtered through an Isopore polycarbonate membrane (EMD Millipore, 10 μm pore size) followed by GF/D filtration (Whatman, 2.7 μm pore size) to retain the 2.7−10 μm fraction and GF/B filtration (EMD Millipore, 1.0 μm pore size) to retain the 1.0−2.7 μm fraction. Each filtration step was made into a separate, combusted filter flask, and the filtration apparatus was rinsed with 1% HCl and ultrapure H_2O between successive filtrations. The POC filters were collected into plastic Petri dishes and stored frozen at −12 °C. Our method removes POC >10 μm in diameter to enable an assessment of the seawater particulate material small enough to transfer into SSA particles, the majority of which have diameters <10 μm.[35] While very little is known about the actual size distribution of seawater particulates transferred into SSA, at least one study has shown that SSA organics chemically resemble POC <10 μm as compared to POC of all sizes,[31] providing validation for our approach.

For DOC collection, two 40 mL aliquots were taken from the communal carboys and GF/F filtered (Whatman, 0.7 μm pore size) into combusted glass vials. The DOC samples were immediately acidified to ~pH 2 with concentrated HCl and stored in a covered box at room temperature.

2.7. Concentration and Isotope Analysis for POC and DOC. Before isotopic analysis, the POC filter samples were processed according to CCE-CalCOFI methods adapted from Bodungen et al.[66] Inorganic carbonate was removed from the samples by acid fumigation in a dessicator for 12 h, and the POC filters were then dried in an oven at 60 °C for 48 h. Subsequently, the POC amount and $\delta^{13}C$ value were analyzed at the SIO Stable Isotope Facility on a Thermo Finnigan DeltaPlus Isotope-Ratio mass spectrometer interfaced with a Costech 4010 elemental combustion analyzer.

Liquid DOC samples were sent to the Jan Veizer Stable Isotope Laboratory in Ottawa, Canada, for $\delta^{13}C$ and concentration analysis. The samples were analyzed on an OI Analytical Aurora Model 1030W Total Organic Carbon (TOC) Analyzer interfaced to a Finnigan DeltaPlus XP Isotope-Ratio mass spectrometer.[67]

2.8. Size-Segregated SSA Collection and Analysis. For size-segregated SSA collection, a stainless-steel sampling apparatus was connected to an aerosol sampling port located ~5 m downstream from the wave breaking region (Figure S1). A y-splitter tube divided the flow in two directions to collect both SSA_{sub} particles and total suspended SSA particles (SSA_{TSP}) onto precombusted quartz fiber filters (Whatman QM-A, 47 mm). Most SSA samples were collected for >40 h to ensure sufficient carbon amounts for isotopic analysis. In addition, field blanks were collected every few days by placing a filter in the sampling apparatus for 10 s to assess the filter handling and analysis carbon blanks (see SI Methods S1). The SSA and field blank filters were collected into plastic Petri dishes and stored frozen at −12 °C until analysis.

https://doi.org/10.1021/acs.est.2c02154
Environ. Sci. Technol. 2022, 56, 9947−9958

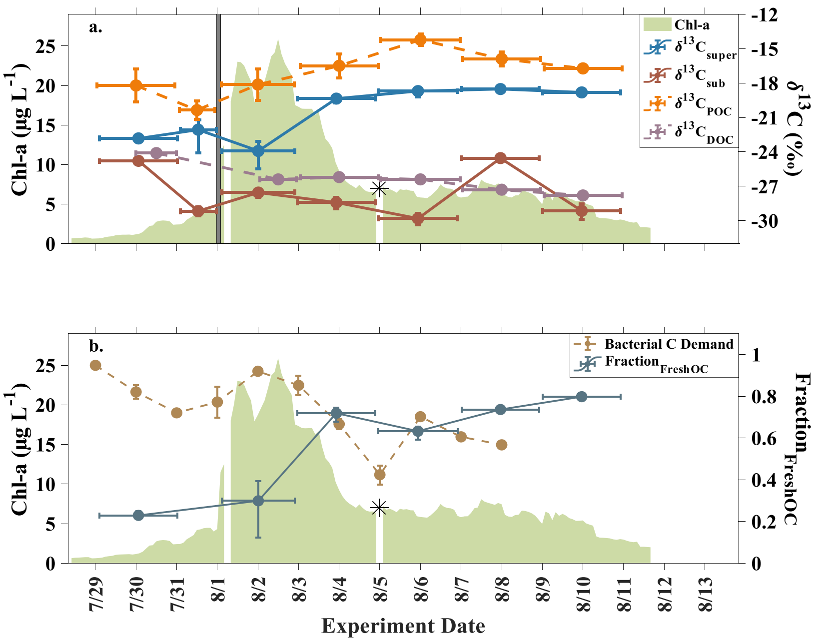

Figure 2. (a) A time series of $\delta^{13}C_{super}$, $\delta^{13}C_{sub}$, $\delta^{13}C_{POC}$, and $\delta^{13}C_{DOC}$ overlaid on the chl-a concentration. A vertical gray line signifies the 10% inoculation as in Figure 1a. (b) A time series showing the inverse relationship between bacterial carbon demand (BCD) and $Fraction_{FreshOC}$ overlaid on the chl-a time series. For both plots, solid lines indicate that samples were collected throughout the entire sampling duration, while the dashed lines signify that the samples were taken at individual time points. Vertical error bars represent measurement uncertainty, while horizontal error bars indicate the collection period or averaging duration for each sample with the data point placed in the center.

Collection of SSA_{sub} was achieved using an URG-2000-30EH cyclone (URG Corp.), which allows particles smaller than the cut point to pass through to the filter while retaining particles larger than the cut point. According to manufacturer settings, this cyclone has a 50% cut point diameter of 1.0 μm at a 50 LPM flow rate. Therefore, SSA was collected out of the wave channel at a total flow rate of 100 LPM using rotameters to keep a 50 LPM flow in both directions and ensure uniform particle distributions. Particles were collected without the use of a drier, as is sometimes done for impactor-based aerosol collections in the marine environment,[13,14,30] so the 1.0 μm cut point for SSA_{sub} applies to the wet particle diameter. Relative humidity was not directly measured for this sampling setup, but based on measurements for similar offline sampling setups during SeaSCAPE, SSA particles were likely collected at a relative humidity of 75−85%.[68]

2.8.1. SSA Sample Analysis. All SSA samples and field blanks were analyzed via a combustion method previously developed in the Thiemens Stable Isotope Laboratory.[27] To convert all carbon species to CO_2, filters were combusted for 3 h at 850 °C in an evacuated quartz tube containing 250 mg of CuO. The total CO_2 yield was measured by capacitance manometry, and $\delta^{13}C$ was analyzed on a MAT 253 Isotope-Ratio mass spectrometer. SSA samples were not acidified to remove carbonates, so OC in SSA refers to the combination of organic carbon, carbonates, and potentially elemental carbon; however, research has shown that carbonates have a minimal effect on the $\delta^{13}C$ of marine aerosols.[16]

The field blank filter measurements were used to correct the SSA_{sub} and SSA_{TSP} carbon amounts and $\delta^{13}C$ values as described in SI Methods S1. The SSA_{super} OC amount was subsequently calculated by taking the difference between the blank-corrected SSA_{TSP} and SSA_{sub} carbon amounts. Likewise, $\delta^{13}C_{super}$ was calculated analogous to eq S1 by realizing that $\delta^{13}C_{TSP}$ is a weighted combination of $\delta^{13}C_{super}$ and $\delta^{13}C_{sub}$.

3. RESULTS AND DISCUSSION

3.1. Biological Progression and Seawater Carbon Dynamics. When discussing the biological progression during the mesocosm study, it is helpful to organize the experiment into three parts based on the experimental phases that occurred: (1) prior to the 10% inoculation (before August 1), (2) highest phytoplankton abundance (August 1−4), and (3) bloom senescence and bacterial growth after the wall scraping (after August 5). Little phytoplankton growth occurred through July 31, prompting the 10% inoculation with the outdoor carboy bloom on August 1. After inoculation with the outdoor carboy bloom and simultaneous augmentation of the algae nutrients to f/2, the wave channel chl-a sharply increased to above 20 μg L^{-1} (Figure 1a) primarily due to the increased growth of diatoms (Figure S2a and SI Methods S2). The chl-a was sustained around this level for 2 days, and the increased primary productivity led to a large drawdown in the dissolved CO_2 concentration (Figure 1a), which has important consequences for the $\delta^{13}C$ value of freshly produced OC in the seawater. After the period of intense biological growth, the biomass accumulated on the wave channel walls was scraped off to allow for a continued radiation flux into the wave channel (asterisk in Figure 1a). Subsequent to the wall scraping, the phytoplankton community shifted to mostly dinoflagellates, and the highest bacteria concentrations were observed in the water column. The bacterial community was dominated by proteobacteria throughout the experiment (Figure S2b), as is the case in many oceanic regimes.[69]

As a result of the biological growth and experimental perturbations, DOC and POC concentrations exhibited vastly different temporal evolutions over the course of the mesocosm experiment (Figure 1b). The DOC (purple) increased by 108 μM following the 10% inoculation, but this increase was entirely due to carbon from the EDTA and vitamins in the f/2 algae nutrient addition.[41] During the bloom growth and senescence phases, the DOC concentration did not increase by more than 23%. The large contribution of EDTA to the seawater carbon raised concerns that it may affect both the organic and isotopic compositions of the nascent SSA. However, LC−MS/MS analysis demonstrated that, after the inoculation, little to no EDTA was detected in the nascent SSA_{TSP}, a combination of SSA_{super} and SSA_{sub} (Figure S3 and SI Methods S3). The minimal contribution of nutrient organics to laboratory-generated SSA has also been confirmed by previous biological experiments using the same nutrient concentrations[41] and indicates that changes to the organic and isotopic composition of nascent SSA in this experiment primarily reflect changes in seawater chemical and biological processes.

Contrary to DOC, POC_{1-10} concentrations were 80−545% higher throughout phytoplankton growth and senescence as compared to the concentration on August 1 right before the 10% inoculation (Figure 1b). This indicates that a significant portion of the POC_{1-10} was freshly produced by biological growth during the experiment. The POC_{1-10} concentrations in Figure 1b are reported in stacked bars separated into two size fractions, 1.0−2.7 μm (red) and 2.7−10 μm (yellow), to show the different particulate sizes available for transfer into SSA_{super}.

3.2. Strong Dissimilarity between $\delta^{13}C_{super}$ and $\delta^{13}C_{sub}$. A comparison of $\delta^{13}C_{super}$ and $\delta^{13}C_{sub}$ in Figure 2a shows that they exhibit distinct isotopic values throughout the entire experiment. The consistently less negative $\delta^{13}C_{super}$ was comparable to previously observed $\delta^{13}C$ values for nascent SSA_{TSP} in a similar biological experiment.[27] Additionally, $\delta^{13}C_{super}$ increased sharply after the chl-a peak, so it appears likely that SSA_{super} organic composition is impacted by seawater biological activity. Unlike $\delta^{13}C_{super}$, $\delta^{13}C_{sub}$ lies well below the values observed for nascent SSA_{TSP}[27] and does not exhibit any obvious relationship with seawater biological activity (chl-a) throughout the bloom. The dissimilar $\delta^{13}C$ values indicate that SSA_{super} and SSA_{sub} differ in their overall organic composition. Furthermore, the disparate temporal evolution of $\delta^{13}C_{super}$ and $\delta^{13}C_{sub}$ during the biological experiment suggests that the SSA_{super} and SSA_{sub} organic compositions are influenced by separate seawater biological and chemical processes. Therefore, our discussion of these results focuses on assessing the biological and physicochemical drivers that may contribute to the distinct differences in $\delta^{13}C$ and organic composition between SSA_{super} and SSA_{sub}.

3.3. A Substantial Biological Influence on SSA_{super} Organic Composition. Examining the experimental time series of $\delta^{13}C$ for POC and DOC, the two seawater carbon pools that contribute to SSA_{super}, provides a good starting point to assess the impact of seawater biological activity on SSA_{super} (Figure 2a). The temporal evolution of $\delta^{13}C_{DOC}$ and $\delta^{13}C_{POC}$ is indicative of variations in bulk organic composition associated with the changes in POC and DOC concentrations. For $\delta^{13}C_{DOC}$, the only significant change was a decrease following the nutrient addition on August 1, but this is likely because commercial EDTA usually has a more negative isotopic value around 29‰.[70] Little variation in $\delta^{13}C_{DOC}$ or DOC concentration was observed after the nutrient addition, indicating that the DOC pool was mostly composed of carbon initially present in the Pacific Ocean source seawater or contributed by the nutrient addition. Conversely, $\delta^{13}C_{POC}$ was higher (less negative) after phytoplankton growth accelerated on August 1, consistent with a lower amount of carbon isotope fractionation that can occur due to changes in seawater temperature or CO_2 availability. The seawater temperature varied by less than 2 °C throughout the entire measurement period,[36] so the higher $\delta^{13}C$ values are likely attributable to lower dissolved CO_2 concentrations during the period of intense phytoplankton growth (Figure 1a).[24,71]

The $\delta^{13}C_{super}$ values have been plotted along with $\delta^{13}C_{POC}$ and $\delta^{13}C_{DOC}$ in Figure 2a to compare the organic composition of SSA_{super} with the seawater carbon pools. As expected for SSA_{super} containing a mixture of seawater POC and DOC, $\delta^{13}C_{super}$ lies in between $\delta^{13}C_{POC}$ and $\delta^{13}C_{DOC}$ for each collection period. This same trend has been previously observed for $\delta^{13}C_{TSP}$ measured during two similar experiments where laboratory phytoplankton blooms were induced by nutrient addition[27] and was also observed for $\delta^{13}C_{TSP}$ in this experiment (Figure S4a). The similarity between $\delta^{13}C_{super}$ and $\delta^{13}C_{TSP}$ is not surprising because SSA_{super} contained >75% of the total SSA carbon for five of the seven collection periods (Figure S4b). Based on the isotopic relationship between SSA and the seawater carbon pools, the prior study used $\delta^{13}C_{DOC}$ and $\delta^{13}C_{POC}$ as approximate endmembers for "aged" and "freshly produced" OC in an isotopic mixing model to estimate the contribution of freshly produced OC to SSA_{TSP}, $Fraction_{FreshOC}$ (eq 3, SI Methods S4).[27] In this study, we have done the same for SSA_{super} with the caveat that "aged" OC refers to the combination of carbon in the initial source seawater and contributed by the nutrient addition.

$$\frac{\delta^{13}C_{SSA} - \delta^{13}C_{DOC}}{\delta^{13}C_{POC} - \delta^{13}C_{DOC}} = \mathrm{Fraction}_{FreshOC} \tag{3}$$

A biological influence on SSA_{super} is immediately apparent from the higher $Fraction_{FreshOC}$ values after the chl-a peak (Figure 2b), but interestingly the increased contribution of freshly produced OC to SSA_{super} is delayed from the chl-a peak by about 2 days. This offset between maximum chl-a and incorporation of freshly produced OC into SSA has been observed before in multiple studies.[27,41,72] Previous studies have posited that the offset may be related to the degradation time scale for freshly produced POC into smaller sizes that efficiently transfer into SSA,[27,73] so in this experiment, we specifically measured POC from 1 to 10 μm, similar to the majority of SSA_{super} particle diameters.[35] Unexpectedly, despite most of the POC_{1-10} being freshly produced (see Section 3.1), the POC_{1-10} concentration in the water column only weakly correlated with the $Fraction_{FreshOC}$ (R^2 = 0.27, Figure S5a). The lack of a significant correlation between the amount of freshly produced OC in the water column and the proportion in SSA_{super} suggests that the secondary biological processing of freshly produced organic material may influence the amount transferred into SSA_{super}.

To assess the secondary processing of freshly produced organic material, we calculated the bacterial carbon demand (BCD) from direct measurements of bacterial production (eq 2, see Section 2.5). In this experiment, a strong inverse relationship existed between the BCD and the $Fraction_{FreshOC}$ values (Figure 2b and Figure S5b, R^2 = 0.88). This points to the alteration of freshly produced organic material by incorporation into bacterial biomass, and especially enhanced remineralization to CO_2, as important mechanisms that may limit the amount of freshly produced OC transported to the ocean surface and transferred into SSA. A bacterial influence on the amount of freshly produced OC available to transfer into SSA_{super} is supported by two additional observations. First,

https://doi.org/10.1021/acs.est.2c02154
Environ. Sci. Technol. 2022, 56, 9947−9958

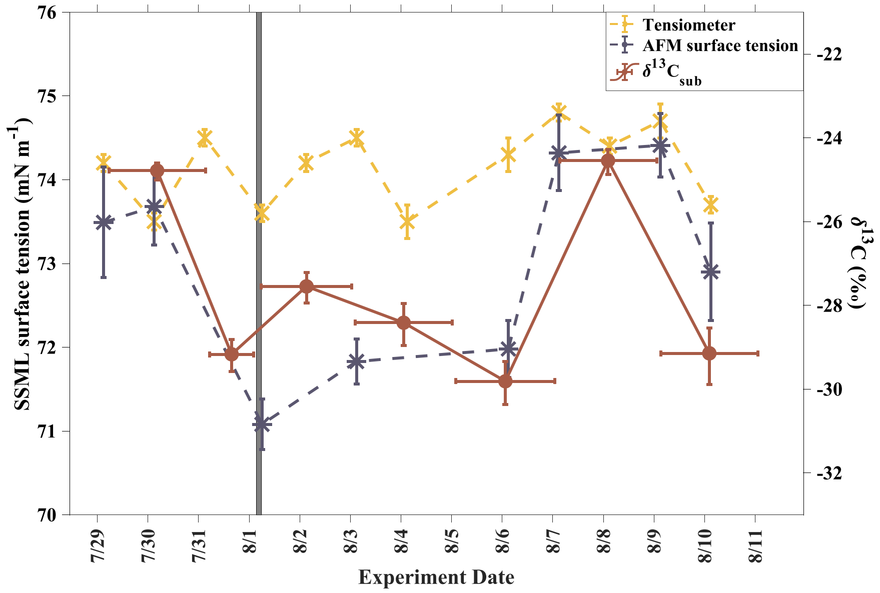

Figure 3. Plots $\delta^{13}C_{sub}$ with SSML surface tension measurements made by both the AFM and tensiometer techniques. The $\delta^{13}C_{sub}$ shows no relation with the tensiometer measurements but closely tracks the AFM-measured surface tension, which probes only the top 0.2−1.5 μm of the SSML sample. Dashed lines indicate that the samples were taken at individual time points, while solid lines signify that the samples were collected throughout the entire sampling duration. Vertical error bars represent measurement uncertainty, while horizontal error bars indicate the collection period or averaging duration for each sample, with the data point placed in the center.

all three peaks in the BCD values, July 29, August 2, and August 6 (Figure 2b), were followed by decreases in POC_{1-10} concentration the next day (Figure 1b). Second, the BCD also exhibited an inverse correlation with the SSA_{super} OC mass percent (Figure S5c), consistent with a lower amount of organic material transferred into SSA_{super} when more OC is being utilized by bacteria in the water column. Taken altogether, these findings suggest that the transfer of freshly produced organic material into SSA_{super} is controlled not just by the amount of freshly produced OC formed from primary productivity, but also by the bacterial assimilation, transformation, and remineralization rates of freshly produced OC. This demonstrates the importance of the complete microbial loop in controlling the organic composition of SSA_{super} and the value of $\delta^{13}C_{super}$.

3.4. Selective Enrichment of Organics in the SSML and SSA_{sub}. In stark contrast to $\delta^{13}C_{super}$, the lower $\delta^{13}C_{sub}$ values were more negative than typical marine, biogenic organic compounds.[74] Instead, the δ^{13}C values for SSA_{sub} resemble those of anthropogenic and terrestrial organic compounds,[75] suggesting that the organic composition of SSA_{sub} produced from coastal seawater may be impacted by anthropogenic activities and terrestrial runoff. Indeed, multiple classes of highly surface-active anthropogenic compounds, including plasticizers, sunscreen products, petrochemicals, and industrial waste, were identified in DOC (<0.2 μm) samples from the initial Pacific Ocean seawater collected for the SeaSCAPE study.[36,76] Many of the anthropogenic compounds in the initial seawater, or their derivatives, continued to persist in the wave channel even after inoculation with the biologically active carboy (Figure S6a), which helps explain why anthropogenic pollutants were also detected in SSA_{sub} during the experiment (Figure S6b).

The presence of anthropogenic compounds was prevalent in both DOC and SSA_{sub}, but SSA_{sub} contained a distinct chemical signature indicative of aliphatic organic species such as oils and surfactants (circled in Figure S6b). Surfactants are often presumed to be preferentially transferred into SSA_{sub} because they are expected to be ubiquitous at the air−sea interface where SSA is formed.[77,78] One method for assessing the presence of surfactants in seawater is by measuring surface tension (see Section 2.4). Pertinently, the surface tension of an SSML sample from the SeaSCAPE study was recently measured by both tensiometer and AFM methods, and the results showed that the AFM-measured surface tension was 2.5 mN m^{-1} lower.[58] The lower AFM-measured surface tension was tentatively attributed to higher surfactant concentrations in the top 0.2−1.5 μm SSML layer probed by the AFM technique. In Figure 3, we have included a more complete time series of surface tension data measured by both the tensiometer and AFM techniques. The tensiometer had a fairly constant surface tension of 73.5−74.5 mN m^{-1}, which is similar to that of pure seawater.[55] Comparatively, the AFM-measured surface tension exhibited a more variable range of 71−74 mN m^{-1}, with the lower values suggesting that, on some days, surfactant levels were elevated in the top ~1 μm of the SSML.

Of particular interest to our work, the $\delta^{13}C_{sub}$ values clearly tracked with the surface tension in the top 0.2−1.5 μm of the SSML as measured by AFM (Figure 3). The lower $\delta^{13}C_{sub}$ values, indicative of a higher anthropogenic contribution, corresponded with decreased AFM-measured SSML surface tension, suggestive of elevated surfactant concentrations. There were also two collection periods (July 29−31 and August 7−9) with higher $\delta^{13}C_{sub}$ values, indicative of a smaller anthropogenic influence on SSA_{sub}, and these same periods had higher AFM-measured surface tension. One explanation consistent with these data is that anthropogenic surfactant levels in the SSML moderated the anthropogenic influence on SSA_{sub}, although this cannot be definitively concluded from our measurements in the absence of concentration or chemical measurements on the SSML. Therefore, from this experiment

https://doi.org/10.1021/acs.est.2c02154
Environ. Sci. Technol. 2022, 56, 9947−9958

alone, we cannot declare a definite relationship between $\delta^{13}C_{sub}$ and SSML surfactant concentrations. However, what does remain clear from our data (Figure 3) is the connection between changes in AFM-measured surface tension, a metric to assess surfactant levels in the topmost 0.2−1.5 μm of the SSML, and $\delta^{13}C_{sub}$, indicative of the bulk organic composition of SSA_{sub}. Taken as a whole, this correspondence may be attributable to elevated anthropogenic surfactant concentrations in the topmost ~1 μm of the SSML, which were then transferred into SSA_{sub} by bubble bursting. Thus, our understanding of organic transfer into SSA_{sub} will benefit from a better characterization of the biological, chemical, and physical factors influencing surfactant concentrations at the air−sea interface.

3.5. Insights into Ocean-Aerosol Transfer of Organic Material. The isotopic measurements made on SSA_{super} and SSA_{sub} in this experiment support the purported motifs for organic transfer into both SSA size fractions (see TOC figure). The isotopic relationships indicated that SSA_{super} likely contained a mixture of bulk DOC and POC, consistent with jet drops formed at the base of the bubble producing SSA_{super} from bulk seawater. Consequently, biologically induced changes in bulk seawater chemical composition will influence the organic composition of SSA_{super} (Figure 2a). Characterizing the impact of seawater biology on SSA_{super} organic composition has substantial implications for climate and precipitation as multiple studies have observed higher SSA ice-nucleating particle (INP) concentrations originating from biologically active seawater.[79,80] Furthermore, a recent study found that the majority of SSA INPs are supermicron particles, and inferred that their enhanced ice-nucleating ability was likely attributable to freshly produced biological material entrained in jet drop SSA_{super} particles.[81] In this experiment, the contribution of freshly produced OC to the total SSA_{super} OC amount was around 25% before significant phytoplankton growth occurred, likely representative of less biologically active oceanic regimes, but increased to >60% after the chl-a peak (Figure 2b). The substantial impact of seawater biology on the proportional contribution of freshly produced OC to SSA_{super} was larger than expected, occurring even though the initial seawater carbon and nutrients comprised the majority of the cumulative bulk seawater POC_{1-10} and DOC (Figure 1b). Previous studies in natural seawater have also found that SSA_{super} contains a large proportion of freshly produced biological material,[26,29] which suggests that there may be additional seawater processes that facilitate the preferential incorporation of freshly produced organic material into SSA_{super}. Recently, Marks et al.[82] provided experimental evidence that a combination of fluid dynamics and electrostatic attractions during bubble ascension can concentrate biological particulate material at the bubble's base, facilitating transfer into jet drop SSA. Looking forward, further research into the physicochemical mechanisms controlling the transfer of particulate material into SSA_{super} will be important to fully elucidate how seawater biological activity influences the organic composition of SSA_{super} and potentially impacts its climate-relevant properties.

For organic transfer into SSA_{sub}, the observed relationship between AFM-measured SSML surface tension and $\delta^{13}C_{sub}$ provides experimental evidence supporting the notion that SSA_{sub} organic composition is influenced by surfactants present in the top ~1 μm of the SSML. Because the AFM probing depth of 0.2−1.5 μm is comparable to the thickness of a bubble's film at the ocean surface,[83] our data are consistent with conventional wisdom that the surface-active organic material present in the top layer of the ocean surface is concentrated on the bubble film and entrained in SSA_{sub} when the bubble bursts. Our experimental findings substantiate the earlier modeling work by Burrows et al.[84] that focused on the top 1 μm of the ocean surface when assessing ocean-aerosol organic transfer. Other ocean-aerosol organic transfer studies have concentrated on measurements of the entire SSML, typically of 50−100 μm thicknesses,[85,86] but our results suggest that organic compounds located in the top ~1−2% of the SSML may be the most relevant for predicting the organic constituents in SSA_{sub}. Therefore, analytical techniques capable of probing morphological and compositional changes in the topmost nanolayers of the seawater surface, such as Brewster angle microscopy, infrared reflection absorption spectroscopy, and sum frequency generation spectroscopy,[87] should provide crucial insight into biological and chemical changes that will affect the organic composition of SSA_{sub}.

■ ASSOCIATED CONTENT

Supporting Information

The Supporting Information is available free of charge at https://pubs.acs.org/doi/10.1021/acs.est.2c02154.

> Description of SSA measurement uncertainties and filter-based calculations (Methods S1); phytoplankton and bacterial community measurements (Methods S2); LC−MS/MS measurements of EDTA (Methods S3); determination of $Fraction_{FreshOC}$ (Methods S4); description of TD-GCxGC-EI-ToF-MS organic speciation measurements (Methods S5); wave channel schematic (Figure S1); phytoplankton and bacterial communities (Figure S2); seawater and SSA_{TSP} EDTA abundance (Figure S3); $\delta^{13}C_{TSP}$ time series and size-segregated OC contributions to SSA (Figure S4); correlation plots demonstrating the relationships between POC, bacteria, and the OC transferred into SSA_{super} (Figure S5); and comparison of organic speciation for seawater DOC and SSA_{sub} (Figure S6) (PDF)

■ AUTHOR INFORMATION

Corresponding Author

Daniel R. Crocker − *Department of Chemistry and Biochemistry, University of California, La Jolla, California 92093, United States;* Present Address: Present address: Department of Earth and Planetary Science, Harvard University, Cambridge, Massachusetts 02138, United States; orcid.org/0000-0002-5297-1103; Phone: (207) 310-8617; Email: dcrocker@fas.harvard.edu

Authors

Chathuri P. Kaluarachchi − *Department of Chemistry, University of Iowa, Iowa City, Iowa 52242, United States;* orcid.org/0000-0003-2538-3952

Ruochen Cao − *Department of Chemistry and Biochemistry, University of California, La Jolla, California 92093, United States*

Julie Dinasquet − *Scripps Institution of Oceanography, University of California, La Jolla, California 92037, United States*

Emily B. Franklin − *Department of Civil and Environmental Engineering, University of California, Berkeley, California 94720, United States;* orcid.org/0000-0002-3568-5359

Clare K. Morris – *Scripps Institution of Oceanography, University of California, La Jolla, California 92037, United States*
Sarah Amiri – *Scripps Institution of Oceanography, University of California, La Jolla, California 92037, United States*
Daniel Petras – *Scripps Institution of Oceanography, University of California, La Jolla, California 92037, United States*
Tran Nguyen – *Scripps Institution of Oceanography, University of California, La Jolla, California 92037, United States*
Ralph R. Torres – *Scripps Institution of Oceanography, University of California, La Jolla, California 92037, United States*
Todd R. Martz – *Scripps Institution of Oceanography, University of California, La Jolla, California 92037, United States*
Francesca Malfatti – *Scripps Institution of Oceanography, University of California, La Jolla, California 92037, United States; University of Trieste, Trieste 34100, Italy; OGS (Istituto Nazionale di Oceanografia e di Geofisica Sperimentale), Trieste 34100, Italy;* orcid.org/0000-0002-0957-9288
Allen H. Goldstein – *Department of Civil and Environmental Engineering and Department of Environmental Science, Policy and Management, University of California, Berkeley, California 94720, United States;* orcid.org/0000-0003-4014-4896
Alexei V. Tivanski – *Department of Chemistry, University of Iowa, Iowa City, Iowa 52242, United States;* orcid.org/0000-0002-1528-2421
Kimberly A. Prather – *Department of Chemistry and Biochemistry, University of California, La Jolla, California 92093, United States; Scripps Institution of Oceanography, University of California, La Jolla, California 92037, United States*
Mark H. Thiemens – *Department of Chemistry and Biochemistry, University of California, La Jolla, California 92093, United States*

Complete contact information is available at:
https://pubs.acs.org/10.1021/acs.est.2c02154

Author Contributions

This manuscript was primarily written by D.R. Crocker. All authors have given approval to the final version of the manuscript.

Notes

The authors declare no competing financial interest.

■ ACKNOWLEDGMENTS

This work was funded by the National Science Foundation Center for Aerosol Impacts on Chemistry of the Environment (NSF-CAICE), a Center for Chemical Innovation (CHE-1801971). First, the authors would like to thank the Editor, Jordi Dachs, and four anonymous reviewers for their insightful feedback that substantially improved this work. The authors thank the entire SeaSCAPE team and especially Dr. Kathryn Mayer, Dr. Jon Sauer, Prof. Timothy Bertram, and Prof. Christopher Cappa for designing and overseeing the campaign. We also thank Lihini Aluwihare and Bruce Deck for their assistance with POC analysis and isotopic measurements. The authors declare no conflicts of interest or financial conflicts in association with this work. LC–MS/MS data are located in MassIVE data repository (massive.ucsd.edu), accession number: MSV000084741. The archived data supporting our conclusions are available from the UC San Diego Library Digital Collections at https://doi.org/10.6075/J0416X7M.

■ REFERENCES

(1) McNeill, V. F. Atmospheric Aerosols: Clouds, Chemistry, and Climate. *Annu. Rev. Chem. Biomol. Eng.* **2017**, *8*, 427–444.
(2) Regayre, L.; Schmale, J.; Johnson, J.; Tatzelt, C.; Baccarini, A.; Henning, S.; Yoshioka, M.; Stratmann, F.; Gysel-Beer, M.; Carslaw, K. The Value of Remote Marine Aerosol Measurements for Constraining Radiative Forcing Uncertainty. *Atmos. Chem. Phys. Discuss.* **2019**, 1–11.
(3) Carslaw, K. S.; Lee, L. A.; Reddington, C. L.; Pringle, K. J.; Rap, A.; Forster, P. M.; Mann, G. W.; Spracklen, D. V.; Woodhouse, M. T.; Regayre, L. A.; Pierce, J. R. Large Contribution of Natural Aerosols to Uncertainty in Indirect Forcing. *Nature* **2013**, *503*, 67–71.
(4) Vignati, E.; Facchini, M. C.; Rinaldi, M.; Scannell, C.; Ceburnis, D.; Sciare, J.; Kanakidou, M.; Myriokefalitakis, S.; Dentener, F.; O'Dowd, C. D. Global Scale Emission and Distribution of Sea-Spray Aerosol: Sea-Salt and Organic Enrichment. *Atmos. Environ.* **2010**, *44*, 670–677.
(5) Rinaldi, M.; Decesari, S.; Finessi, E.; Giulianelli, L.; Carbone, C.; Fuzzi, S.; O'Dowd, C. D.; Ceburnis, D.; Facchini, M. C. Primary and Secondary Organic Marine Aerosol and Oceanic Biological Activity: Recent Results and New Perspectives for Future Studies. *Adv. Meteorol.* **2010**, *2010*, 1–10.
(6) Quinn, P. K.; Collins, D. B.; Grassian, V. H.; Prather, K. A.; Bates, T. S. Chemistry and Related Properties of Freshly Emitted Sea Spray Aerosol. *Chem. Rev.* **2015**, *115*, 4383–4399.
(7) Aswini, A. R.; Hegde, P.; Aryasree, S.; Girach, I. A.; Nair, P. R. Continental Outflow of Anthropogenic Aerosols over Arabian Sea and Indian Ocean during Wintertime: ICARB-2018 Campaign. *Sci. Total Environ.* **2020**, *712*, No. 135214.
(8) Wang, Y.; Wang, M.; Zhang, R.; Ghan, S. J.; Lin, Y.; Hu, J.; Pan, B.; Levy, M.; Jiang, J. H.; Molina, M. J. Assessing the Effects of Anthropogenic Aerosols on Pacific Storm Track Using a Multiscale Global Climate Model. *PNAS* **2014**, *111*, 6894–6899.
(9) Brooks, S. D.; Thornton, D. C. O. Marine Aerosols and Clouds. *Annu. Rev. Mar. Sci.* **2018**, *10*, 289–313.
(10) Gaston, C.; Cahill, J.; Collins, D.; Suski, K.; Ge, J.; Barkley, A.; Prather, K. The Cloud Nucleating Properties and Mixing State of Marine Aerosols Sampled along the Southern California Coast. *Atmosphere* **2018**, *9*, 52.
(11) Chesselet, R.; Fontugne, M.; Buat-Menard, P.; Esat, U.; Lambert, C. E. The Origin of Particulate Organic Carbon in the Marine Atmosphere as Indicated by Its Stable Carbon Isotopic Composition. 1981, *8* (4), 345–348, DOI: 10.1029/GL008i004p00345.
(12) Cachier, H.; Buat-Ménard, P.; Fontugne, M.; Chesselet, R. Long-range Transport of Continentally-derived Particulate Carbon in the Marine Atmosphere: Evidence from Stable Carbon Isotope Studies. *Tellus B* **1986**, *38B*, 161–177.
(13) Turekian, V. C.; Macko, S. A.; Keene, W. C. Concentrations, Isotopic Compositions, and Sources of Size-Resolved, Particulate Organic Carbon and Oxalate in near-Surface Marine Air at Bermuda during Spring. *J. Geophys. Res. Atmos.* **2003**, *108* (), DOI: 10.1029/2002jd002053.
(14) Miyazaki, Y.; Kawamura, K.; Sawano, M. Size Distributions of Organic Nitrogen and Carbon in Remote Marine Aerosols: Evidence of Marine Biological Origin Based on Their Isotopic Ratios. *Geophys. Res. Lett.* **2010**, *37* (), DOI: 10.1029/2010GL042483.
(15) Ceburnis, D.; Garbaras, A.; Szidat, S.; Rinaldi, M.; Fahrni, S.; Perron, N.; Wacker, L.; Leinert, S.; Remeikis, V.; Facchini, M. C.; Prévôt, A. S. H.; Jennings, S. G.; Ramonet, M.; O'Dowd, C. D. Quantification of the Carbonaceous Matter Origin in Submicron

Marine Aerosol by 13C and 14C Isotope Analysis. *Atmos. Chem. Phys.* **2011**, *11*, 8593−8606.
(16) Kundu, S.; Kawamura, K. Seasonal Variations of Stable Carbon Isotopic Composition of Bulk Aerosol Carbon from Gosan Site, Jeju Island in the East China Sea. *Atmos. Environ.* **2014**, *94*, 316−322.
(17) Aggarwal, S. G.; Kawamura, K. Molecular Distributions and Stable Carbon Isotopic Compositions of Dicarboxylic Acids and Related Compounds in Aerosols from Sapporo, Japan: Implications for Photochemical Aging during Long-Range Atmospheric Transport. *J. Geophys. Res. Atmos.* **2008**, *113*, 1−13.
(18) Shank, L. M.; Howell, S.; Clarke, A. D.; Freitag, S.; Brekhovskikh, V.; Kapustin, V.; McNaughton, C.; Campos, T.; Wood, R. Organic Matter and Non-Refractory Aerosol over the Remote Southeast Pacific: Oceanic and Combustion Sources. *Atmos. Chem. Phys.* **2012**, *12*, 557−576.
(19) Miyazaki, Y.; Yamashita, Y.; Kawana, K.; Tachibana, E.; Kagami, S.; Mochida, M.; Suzuki, K.; Nishioka, J. Chemical Transfer of Dissolved Organic Matter from Surface Seawater to Sea Spray Water-Soluble Organic Aerosol in the Marine Atmosphere. *Sci. Rep.* **2018**, *8*, 1−10.
(20) Verdugo, P.; Alldredge, A. L.; Azam, F.; Kirchman, D. L.; Passow, U.; Santschi, P. H. The Oceanic Gel Phase: A Bridge in the DOM-POM Continuum. *Mar. Chem.* **2004**, *92*, 67−85.
(21) Kharbush, J. J.; Close, H. G.; Van Mooy, B. A. S.; Arnosti, C.; Smittenberg, R. H.; Le Moigne, F. A. C.; Mollenhauer, G.; Scholz-Böttcher, B.; Obreht, I.; Koch, B. P.; Becker, K. W.; Iversen, M. H.; Mohr, W. Particulate Organic Carbon Deconstructed: Molecular and Chemical Composition of Particulate Organic Carbon in the Ocean. *Front. Mar. Sci.* **2020**, *7*, 1−10.
(22) McNichol, A. P.; Aluwihare, L. I. The Power of Radiocarbon in Biogeochemical Studies of the Marine Carbon Cycle: Insights from Studies of Dissolved and Particulate Organic Carbon (DOC and POC). *Chem. Rev.* **2007**, *107*, 443−466.
(23) Beaupré, S. R.; Kieber, D. J.; Keene, W. C.; Long, M. S.; Maben, J. R.; Lu, X.; Zhu, Y.; Frossard, A. A.; Kinsey, J. D.; Duplessis, P.; Chang, R. Y. W.; Bisgrove, J. Oceanic Efflux of Ancient Marine Dissolved Organic Carbon in Primary Marine Aerosol. *Sci. Adv.* **2019**, *5*, No. eaax6535.
(24) Kukert, H.; Riebesell, U. Phytoplankton Carbon Isotope Fractionation during a Diatom Spring Bloom in a Norwegian Fjord. *Mar. Ecol. Prog. Ser.* **1998**, *173*, 127−138.
(25) Esposito, M.; Achterberg, E. P.; Bach, L. T.; Connelly, D. P.; Riebesell, U.; Taucher, J. Application of Stable Carbon Isotopes in a Subtropical North Atlantic MesocosmStudy: A New Approach to Assess CO2 Effects on the Marine Carbon Cycle. *Front. Mar. Sci.* **2019**, *6*, 1−17.
(26) Ceburnis, D.; Masalaite, A.; Ovadnevaite, J.; Garbaras, A.; Remeikis, V.; Maenhaut, W.; Claeys, M.; Sciare, J.; Baisnée, D.; O'Dowd, C. D. Stable Isotopes Measurements Reveal Dual Carbon Pools Contributing to Organic Matter Enrichment in Marine Aerosol. *Sci. Rep.* **2016**, *6*, 1−6.
(27) Crocker, D. R.; Hernandez, R. E.; Huang, H. D.; Pendergraft, M. A.; Cao, R.; Dai, J.; Morris, C. K.; Deane, G. B.; Prather, K. A.; Thiemens, M. H. Biological Influence on D13C and Organic Composition of Nascent Sea Spray Aerosol. *ACS Earth Sp. Chem.* **2020**, *4*, 1686−1699.
(28) Miyazaki, Y.; Kawamura, K.; Jung, J.; Furutani, H.; Uematsu, M. Latitudinal Distributions of Organic Nitrogen and Organic Carbon in Marine Aerosols over the Western North Pacific. *Atmos. Chem. Phys.* **2011**, *11*, 3037−3049.
(29) Rastelli, E.; Corinaldesi, C.; Dell'anno, A.; Lo Martire, M.; Greco, S.; Cristina Facchini, M.; Rinaldi, M.; O'Dowd, C.; Ceburnis, D.; Danovaro, R. Transfer of Labile Organic Matter and Microbes from the Ocean Surface to the Marine Aerosol: An Experimental Approach. *Sci. Rep.* **2017**, *7*, 11475.
(30) Cavalli, F.; Facchini, M. C.; Decesari, S.; Mircea, M.; Emblico, L.; Fuzzi, S.; Ceburnis, D.; Yoon, Y. J.; O'Dowd, C. D.; Putaud, J. P.; Dell'Acqua, A. Advances in Characterization of Size-Resolved Organic Matter in Marine Aerosol over the North Atlantic. *J. Geophys. Res. D Atmos.* **2004**, *109*, 1−14.
(31) Facchini, M. C.; Rinaldi, M.; Decesari, S.; Carbone, C.; Finessi, E.; Mircea, M.; Fuzzi, S.; Ceburnis, D.; Flanagan, R.; Nilsson, E. D.; de Leeuw, G.; Martino, M.; Woeltjen, J.; O'Dowd, C. D. Primary Submicron Marine Aerosol Dominated by Insoluble Organic Colloids and Aggregates. *Geophys. Res. Lett.* **2008**, *35* (), DOI: 10.1029/2008GL034210.
(32) Wang, X.; Sultana, C. M.; Trueblood, J.; Hill, T. C. J.; Malfatti, F.; Lee, C.; Laskina, O.; Moore, K. A.; Beall, C. M.; McCluskey, C. S.; Cornwell, G. C.; Zhou, Y.; Cox, J. L.; Pendergraft, M. A.; Santander, M. V.; Bertram, T. H.; Cappa, C. D.; Azam, F.; DeMott, P. J.; Grassian, V. H.; Prather, K. A. Microbial Control of Sea Spray Aerosol Composition: A Tale of Two Blooms. *ACS Cent. Sci.* **2015**, *1*, 124−131.
(33) Wurl, O.; Miller, L.; Röttgers, R.; Vagle, S. The Distribution and Fate of Surface-Active Substances in the Sea-Surface Microlayer and Water Column. *Mar. Chem.* **2009**, *115*, 1−9.
(34) Mustaffa, N. I. H.; Latif, M. T.; Ali, M. M. Distribution of Surfactants in Sea-Surface Microlayer and Atmospheric Aerosols at Selected Coastal Area of Peninsular Malaysia. *AIP Conf. Proc.* , *2013* (,), 625−631, DOI: 10.1063/1.4858724.
(35) Prather, K. A.; Bertram, T. H.; Grassian, V. H.; Deane, G. B.; Stokes, M. D.; DeMott, P. J.; Aluwihare, L. I.; Palenik, B. P.; Azam, F.; Seinfeld, J. H.; Moffet, R. C.; Molina, M. J.; Cappa, C. D.; Geiger, F. M.; Roberts, G. C.; Russell, L. M.; Ault, A. P.; Baltrusaitis, J.; Collins, D. B.; Corrigan, C. E.; Cuadra-Rodriguez, L. A.; Ebben, C. J.; Forestieri, S. D.; Guasco, T. L.; Hersey, S. P.; Kim, M. J.; Lambert, W. F.; Modini, R. L.; Mui, W.; Pedler, B. E.; Ruppel, M. J.; Ryder, O. S.; Schoepp, N. G.; Sullivan, R. C.; Zhao, D. Bringing the Ocean into the Laboratory to Probe the Chemical Complexity of Sea Spray Aerosol. *PNAS* **2013**, *110*, 7550−7555.
(36) Sauer, J. S.; Mayer, K. J.; Lee, C.; Alves, M. R.; Amiri, S.; Bahaveolos, C.; Barnes, E. B.; Crocker, D. R.; Dinasquet, J.; Garofalo, L. A.; Kaluarachchi, C. P.; Dang, D.; Kilgour, D.; Mael, L.; Mitts, B. A.; Moon, D. R.; Morris, C. K.; Moore, A. N.; Ni, C.-M.; Pendergraft, M. A.; Petras, D.; Simpson, R.; Smith, S.; Tumminello, P. R.; Walker, J. L.; DeMott, P. J.; Farmer, D. K.; Goldstein, A. H.; Grassian, V. H.; Jaffe, J. S.; Malfatti, F.; Martz, T. R.; Slade, J.; Tivanski, A. V.; Bertram, T. H.; Cappa, C. D.; Prather, K. A. The Sea Spray Chemistry and Particle Evolution Study (SeaSCAPE): Overview and Experimental Methods. *Environ. Sci. Process. Impacts* **2022**, *24*, 290−315.
(37) Guillard, R. R. L.; Ryther, J. H. Studies of Marine Planktonic Diatoms I. Cyclotella nana Hustedt, and Detonula confervacea. *Can. J. Microbiol.* **1962**, *8*, 229−239.
(38) Bouvet, M.; Hoepffner, N.; Dowell, M. D. Parameterization of a Spectral Solar Irradiance Model for the Global Ocean Using Multiple Satellite Sensors. *J. Geophys. Res. Ocean.* **2002**, *107*, 8-1.
(39) Quinn, P. K.; Bates, T. S.; Schulz, K. S.; Coffman, D. J.; Frossard, A. A.; Russell, L. M.; Keene, W. C.; Kieber, D. J. Contribution of Sea Surface Carbon Pool to Organic Matter Enrichment in Sea Spray Aerosol. *Nat. Geosci.* **2014**, *7*, 228−232.
(40) Sciare, J.; Favez, O.; Sarda-Estève, R.; Oikonomou, K.; Cachier, H.; Kazan, V. Long-Term Observations of Carbonaceous Aerosols in the Austral Ocean Atmosphere: Evidence of a Biogenic Marine Organic Source. *J. Geophys. Res. Atmos.* **2009**, *114*, 1−10.
(41) Lee, C.; Sultana, C. M.; Collins, D. B.; Santander, M. V.; Axson, J. L.; Malfatti, F.; Cornwell, G. C.; Grandquist, J. R.; Deane, G. B.; Stokes, M. D.; Azam, F.; Grassian, V. H.; Prather, K. A. Advancing Model Systems for Fundamental Laboratory Studies of Sea Spray Aerosol Using the Microbial Loop. *J. Phys. Chem. A* **2015**, *119*, 8860−8870.
(42) Engel, A.; Schulz, K. G.; Riebesell, U.; Bellerby, R.; Delille, B.; Schartau, M. Effects of CO2 on Particle Size Distribution and Phytoplankton Abundance during a Mesocosm Bloom Experiment (PeECE II). *Biogeosciences* **2008**, *5*, 509−521.
(43) Gazeau, F.; Sallon, A.; Maugendre, L.; Louis, J.; Dellisanti, W.; Gaubert, M.; Lejeune, P.; Gobert, S.; Borges, A. V.; Harlay, J.; Champenois, W.; Alliouane, S.; Taillandier, V.; Louis, F.; Obolensky,

G.; Grisoni, J. M.; Guieu, C. First Mesocosm Experiments to Study the Impacts of Ocean Acidification on Plankton Communities in the NW Mediterranean Sea (MedSeA Project). *Estuar. Coast. Shelf Sci.* **2017**, *186*, 11−29.

(44) Tumminello, P. R.; James, R. C.; Kruse, S.; Kawasaki, A.; Cooper, A.; Guadalupe-Diaz, I.; Zepeda, K. L.; Crocker, D. R.; Mayer, K. J.; Sauer, J. S.; Lee, C.; Prather, K. A.; Slade, J. H. Evolution of Sea Spray Aerosol Particle Phase State across a Phytoplankton Bloom. *ACS Earth Sp. Chem.* **2021**, *5*, 2995−3007.

(45) Kilgour, D.; Novak, G.; Sauer, J.; Moore, A.; Dinasquet, J.; Amiri, S.; Franklin, E.; Mayer, K.; Winter, M.; Morris, C.; Price, T.; Malfatti, F.; Crocker, D.; Lee, C.; Cappa, C.; Goldstein, A.; Prather, K.; Bertram, T. Marine Gas-Phase Sulfur Emissions during an Induced Phytoplankton Bloom. *Atmos. Chem. Phys.* **2021**, 1−24.

(46) Crocker, D. R.; Deane, G. B.; Cao, R.; Santander, M. V.; Morris, C. K.; Mitts, B. A.; Dinasquet, J.; Amiri, S.; Malfatti, F.; Prather, K. A.; Thiemens, M. H. Biologically Induced Changes in the Partitioning of Submicron Particulates Between Bulk Seawater and the Sea Surface Microlayer. *Geophys. Res. Lett.* **2022**, *49*, 1−11.

(47) Holm-Hansen, O.; Lorenzen, C. J.; Holmes, R. W.; Strickland, J. D. H. Fluorometric Determination of Chlorophyll. *ICES J. Mar. Sci.* **1965**, *30*, 3−15.

(48) Bandstra, L.; Hales, B.; Takahashi, T. High-Frequency Measurements of Total CO2: Method Development and First Oceanographic Observations. *Mar. Chem.* **2006**, *100*, 24−38.

(49) Hales, B.; Chipman, D.; Takahashi, T. High-Frequency Measurement of Partial Pressure and Total Concentration of Carbon Dioxide in Seawater Using Microporous Hydrophobic Membrane Contactors. *Limnol. Oceanogr. Methods* **2004**, *2*, 356−364.

(50) Cunliffe, M.; Wurl, O. Sampling the Sea Surface Microlayer. 2015, 255−261, DOI: 10.1007/8623_2015_83.

(51) Carlson, D. J. Surface Microlayer Phenolic Enrichments Indicate Sea Surface Slicks. *Nature* **1982**, *296*, 426−429.

(52) Cunliffe, M.; Engel, A.; Frka, S.; Gašparović, B. Ž.; Guitart, C.; Murrell, J. C.; Salter, M.; Stolle, C.; Upstill-Goddard, R.; Wurl, O. Sea Surface Microlayers: A Unified Physicochemical and Biological Perspective of the Air-Ocean Interface. *Prog. Oceanogr.* **2013**, *109*, 104−116.

(53) Nayar, K. G.; Panchanathan, D.; McKinley, G. H.; Lienhard, J. H.; Liehard, V. Surface Tension of Seawater. *J. Phys. Chem. Ref. Data* **2014**, *43*, No. 043103.

(54) Hendrickson, B. N.; Brooks, S. D.; Thornton, D. C. O.; Moore, R. H.; Crosbie, E.; Ziemba, L. D.; Carlson, C. A.; Baetge, N.; Mirrielees, J. A.; Alsante, A. N. Role of Sea Surface Microlayer Properties in Cloud Formation. *Front. Mar. Sci.* **2021**, *7*, 1−20.

(55) Frossard, A. A.; Gérard, V.; Duplessis, P.; Kinsey, J. D.; Lu, X.; Zhu, Y.; Bisgrove, J.; Maben, J. R.; Long, M. S.; Chang, R. Y. W.; Beaupré, S. R.; Kieber, D. J.; Keene, W. C.; Nozière, B.; Cohen, R. C. Properties of Seawater Surfactants Associated with Primary Marine Aerosol Particles Produced by Bursting Bubbles at a Model Air-Sea Interface. *Environ. Sci. Technol.* **2019**, *53*, 9407−9417.

(56) Padday, J. F.; Pitt, A. R.; Pashley, R. M. Menisci at a Free Liquid Surface: Surface Tension from the Maximum Pull on a Rod. *J. Chem. Soc. Faraday Trans. 1* **1975**, *71*, 1919−1931.

(57) Morris, H. S.; Grassian, V. H.; Tivanski, A. V. Humidity-Dependent Surface Tension Measurements of Individual Inorganic and Organic Submicrometre Liquid Particles. *Chem. Sci.* **2015**, *6*, 3242−3247.

(58) Kaluarachchi, C. P.; Lee, H. D.; Lan, Y.; Lansakara, T. I.; Tivanski, A. V. Surface Tension Measurements of Aqueous Liquid-Air Interfaces Probed with Microscopic Indentation. *Langmuir* **2021**, *37*, 2457−2465.

(59) Gasol, J. M.; Del Giorgio, P. A. Using Flow Cytometry for Counting Natural Planktonic Bacteria and Understanding the Structure of Planktonic Bacterial Communities. *Sci.* **Mar. 2000**, *64*, 197−224.

(60) Marie, D.; Partensky, F.; Jacquet, S.; Vaulot, D. Enumeration and Cell Cycle Analysis of Natural Populations of Marine Picoplankton by Flow Cytometry Using the Nucleic Acid Stain SYBR Green I. *Appl. Environ. Microbiol.* **1997**, *63*, 186−193.

(61) Noble, R. T.; Fuhrman, J. A. Use of SYBR Green I for Rapid Epifluorescence Counts of Marine Viruses and Bacteria. *Aquat. Microb. Ecol.* **1998**, *14*, 113−118.

(62) Kirchman, D.; K'nees, E.; Hodson, R. Leucine Incorporation and Its Potential as a Measure of Protein Synthesis by Bacteria in Natural Aquatic Systems. *Appl. Environ. Microbiol.* **1985**, *49*, 599−607.

(63) Smith, D.; Azam, F. A Simple, Economical Method for Measuring Bacterial Protein Synthesis Rates in Seawater Using. *Mar. Microb. food webs* **1992**, *6*, 107−114.

(64) Simon, M.; Azam, F. Protein Content and Protein Synthesis Rates of Planktonic Marine Bacteria. *Mar. Ecol. Prog. Ser.* **1989**, *51*, 201−213.

(65) del Giorgio, P. A.; Cole, J. J. Bacterial Growth Efficiency in Natural Aquatic Systems. *Annu. Rev. Ecol. Syst.* **1998**, *29*, 503−541.

(66) Bodungen, B. V.; Wunsch, M.; Fürderer, H. Sampling and Analysis of Suspended and Sinking Particles in the Northern North Atlantic. *Geophysica.* **2013**, DOI: 10.1029/gm063p0047.

(67) Lalonde, K.; Middlestead, P.; Gélinas, Y. Automation of 13C/12C Ratio Measurement for Freshwater and Seawater DOC Using High Temperature Combustion. *Limnol. Oceanogr. Methods* **2014**, *12*, 816−829.

(68) Angle, K. J.; Crocker, D. R.; Simpson, R. M. C.; Mayer, K. J.; Garofalo, L. A.; Moore, A. N.; Mora Garcia, S. L.; Or, V. W.; Srinivasan, S.; Farhan, M.; Sauer, J. S.; Lee, C.; Pothier, M. A.; Farmer, D. K.; Martz, T. R.; Bertram, T. H.; Cappa, C. D.; Prather, K. A.; Grassian, V. H. Acidity across the Interface from the Ocean Surface to Sea Spray Aerosol. *PNAS* **2021**, *118* (), DOI: 10.1073/pnas.2018397118.

(69) Bolaños, L. M.; Choi, C. J.; Worden, A. Z.; Baetge, N.; Carlson, C. A.; Giovannoni, S. Seasonality of the Microbial Community Composition in the North Atlantic. *Front. Mar. Sci.* **2021**, *8*, 1−16.

(70) Käkelä, A.; Furness, R. W.; Kelly, A.; Strandberg, U.; Waldron, S.; Käkelä, R. Fatty Acid Signatures and Stable Isotopes as Dietary Indicators in North Sea Seabirds. *Mar. Ecol. Prog. Ser.* **2007**, *342*, 291−301.

(71) Ostrom, N. E.; Macko, S. A.; Deibel, D.; Thompson, R. J. Seasonal Variation in the Stable Carbon and Nitrogen Isotope Biogeochemistry of a Coastal Cold Ocean Environment. *Geochim. Cosmochim. Acta* **1997**, *61*, 2929−2942.

(72) O'Dowd, C.; Ceburnis, D.; Ovadnevaite, J.; Bialek, J.; Stengel, D. B.; Zacharias, M.; Nitschke, U.; Connan, S.; Rinaldi, M.; Fuzzi, S.; Decesari, S.; Cristina Facchini, M.; Marullo, S.; Santoleri, R.; Dell'anno, A.; Corinaldesi, C.; Tangherlini, M.; Danovaro, R. Connecting Marine Productivity to Sea-Spray via Nanoscale Biological Processes: Phytoplankton Dance or Death Disco? *Sci. Rep.* **2015**, *5*, 1−11.

(73) Rinaldi, M.; Fuzzi, S.; Decesari, S.; Marullo, S.; Santoleri, R.; Provenzale, A.; Von Hardenberg, J.; Ceburnis, D.; Vaishya, A.; O'Dowd, C. D.; Facchini, M. C. Is Chlorophyll-a the Best Surrogate for Organic Matter Enrichment in Submicron Primary Marine Aerosol? *J. Geophys. Res. Atmos.* **2013**, *118*, 4964−4973.

(74) Loh, A. N.; Bauer, J. E.; Druffel, E. R. M. Variable Ageing and Storage of Dissolved Organic Components in the Open Ocean. *Nature* **2004**, *430*, 877−881.

(75) Mudge, S. M.; Meier-Augenstein, W.; Eadsforth, C.; DeLeo, P. What Contribution Do Detergent Fatty Alcohols Make to Sewage Discharges and the Marine Environment? *J. Environ. Monit.* **2010**, *12*, 1846−1856.

(76) Franklin, E. B.; Alves, M. R.; Moore, A. N.; Kilgour, D. B.; Novak, G. A.; Mayer, K.; Sauer, J. S.; Weber, R. J.; Dang, D.; Winter, M.; Lee, C.; Cappa, C. D.; Bertram, T. H.; Prather, K. A.; Grassian, V. H.; Goldstein, A. H. Atmospheric Benzothiazoles in a Coastal Marine Environment. *Environ. Sci. Technol.* **2021**, *55*, 15705−15714.

(77) Cochran, R. E.; Laskina, O.; Jayarathne, T.; Laskin, A.; Laskin, J.; Lin, P.; Sultana, C.; Lee, C.; Moore, K. A.; Cappa, C. D.; Bertram, T. H.; Prather, K. A.; Grassian, V. H.; Stone, E. A. Analysis of Organic

Anionic Surfactants in Fine and Coarse Fractions of Freshly Emitted Sea Spray Aerosol. *Environ. Sci. Technol.* **2016**, *50*, 2477−2486.
(78) Schmitt-Kopplin, P.; Liger-Belair, G.; Koch, B. P.; Flerus, R.; Kattner, G.; Harir, M.; Kanawati, B.; Lucio, M.; Tziotis, D.; Hertkorn, N.; Gebefügi, I. Dissolved Organic Matter in Sea Spray: A Transfer Study from Marine Surface Water to Aerosols. *Biogeosciences* **2012**, *9*, 1571−1582.
(79) Creamean, J. M.; Cross, J. N.; Pickart, R.; McRaven, L.; Lin, P.; Pacini, A.; Hanlon, R.; Schmale, D. G.; Ceniceros, J.; Aydell, T.; Colombi, N.; Bolger, E.; DeMott, P. J. Ice Nucleating Particles Carried From Below a Phytoplankton Bloom to the Arctic Atmosphere. *Geophys. Res. Lett.* **2019**, *46*, 8572−8581.
(80) DeMott, P. J.; Hill, T. C. J.; McCluskey, C. S.; Prather, K. A.; Collins, D. B.; Sullivan, R. C.; Ruppel, M. J.; Mason, R. H.; Irish, V. E.; Lee, T.; Hwang, C. Y.; Rhee, T. S.; Snider, J. R.; McMeeking, G. R.; Dhaniyala, S.; Lewis, E. R.; Wentzell, J. J. B.; Abbatt, J.; Lee, C.; Sultana, C. M.; Ault, A. P.; Axson, J. L.; Martinez, M. D.; Venero, I.; Santos-Figueroa, G.; Stokes, M. D.; Deane, G. B.; Mayol-Bracero, O. L.; Grassian, V. H.; Bertram, T. H.; Bertram, A. K.; Moffett, B. F.; Franc, G. D. Sea Spray Aerosol as a Unique Source of Ice Nucleating Particles. *PNAS* **2016**, *113*, 5797−5803.
(81) Mitts, B. A.; Wang, X.; Lucero, D. D.; Beall, C. M.; Deane, G. B.; DeMott, P. J.; Prather, K. A. Importance of Supermicron Ice Nucleating Particles in Nascent Sea Spray. *Geophys. Res. Lett.* **2021**, *48* (), DOI: 10.1029/2020GL089633.
(82) Marks, R.; Górecka, E.; McCartney, K.; Borkowski, W. Rising Bubbles as Mechanism for Scavenging and Aerosolization of Diatoms. *J. Aerosol Sci.* **2019**, *128*, 79−88.
(83) Modini, R. L.; Russell, L. M.; Deane, G. B.; Stokes, M. D. Effect of Soluble Surfactant on Bubble Persistence and Bubble-Produced Aerosol Particles. *J. Geophys. Res. Atmos.* **2013**, *118*, 1388−1400.
(84) Burrows, S. M.; Ogunro, O.; Frossard, A. A.; Russell, L. M.; Rasch, P. J.; Elliott, S. M. A Physically Based Framework for Modeling the Organic Fractionation of Sea Spray Aerosol from Bubble Film Langmuir Equilibria. *Atmos. Chem. Phys.* **2014**, *14*, 13601−13629.
(85) Van Pinxteren, M.; Barthel, S.; Fomba, K. W.; Müller, K.; Von Tümpling, W.; Herrmann, H. The Influence of Environmental Drivers on the Enrichment of Organic Carbon in the Sea Surface Microlayer and in Submicron Aerosol Particles − Measurements from the Atlantic Ocean. *Elementa* **2017**, *5* (). DOI: 10.1525/elementa.225.
(86) Engel, A.; Bange, H. W.; Cunliffe, M.; Burrows, S. M.; Friedrichs, G.; Galgani, L.; Herrmann, H.; Hertkorn, N.; Johnson, M.; Liss, P. S.; Quinn, P. K.; Schartau, M.; Soloviev, A.; Stolle, C.; Upstill-Goddard, R. C.; van Pinxteren, M.; Zäncker, B. The Ocean's Vital Skin: Toward an Integrated Understanding of the Sea Surface Microlayer. *Front. Mar. Sci.* **2017**, *4*, 1−14.
(87) Rogers, M. M.; Neal, J. F.; Saha, A.; Algarni, A. S.; Hill, T. C. J.; Allen, H. C. The Ocean's Elevator: Evolution of the Air-Seawater Interface during a Small-Scale Algal Bloom. *ACS Earth Sp. Chem.* **2020**, *4*, 2347−2357.

https://doi.org/10.1021/acs.est.2c02154
Environ. Sci. Technol. 2022, 56, 9947−9958